Bulletin of the Mineral Research and Exploration

http://bulletin.mta.gov.tr

Uncertainty-volume fractal model for delineating copper mineralization controllers using geostatistical simulation in Nohkouhi volcanogenic massive sulfide deposit, Central Iran

Saeid HAJSADEGHI[a], Omid ASGHARI[b*], Mirsaleh MIRMOHAMMADI[a], Peyman AFZAL[c] and Seyed Ahmad MESHKANI[a]

[a]*School of Mining Engineering, University of Tehran, Iran.*
[b]*Simulation and Data Processing Laboratory, School of Mining Engineering, University of Tehran, Tehran, Iran.*
[c]*Department of Mining Engineering, South Tehran Branch, Islamic Azad University, Tehran, Iran.*

Research Article

Keywords:
Sequential Gaussian simulation, Sequential indicator simulation, Concentration–volume fractal modeling, Uncertainty-volume fractal modeling, Volcanogenic massive sulfide, Nohkouhi copper deposit.

Received Date: 29.07.2018
Accepted Date: 14.11.2018

ABSTRACT

The aim of this study was to delineate copper mineralization controllers in Nohkouhi volcanogenic massive sulfide (VMS) deposit by using geostatistical and fractal simulation. In this study, concentration-volume (C-V) fractal model has been used to indicate various copper populations related to different host rocks and copper minerals. Accordingly, uncertainty-volume (U-V) fractal model was applied to probability values achieved through sequential indicator simulation (SIS). Copper ores of Nohkouhi deposit including chalcopyrite and malachite were simulated in 30 realizations. The U-V fractal model obtained by using a probability map was divided into four probability zones (high, moderate, low, and very low) for copper minerals. Furthermore, copper grades were simulated for 10 times by sequential Gaussian simulation (SGS). Combination of C–V and U-V fractal modeling resulted in a hybrid method which could be properly employed to determinate various mineralization zones based on the relationship between quantitative (e.g. copper grade) and qualitative (e.g. copper minerals) variables. Moreover, integrating the results of C–V and U-V fractal modeling with the most frequent occurrence of rock type modeling helps identify copper mineralization controllers in a VMS deposit.

1. Introduction

Fractal models, presented by Mandelbrot (1983), has been used in many different cases to explain geological and mineralization processes. Considering spatial information of mineral deposit data, it can be noted that fractal models are useful tools which reveal the relationships among geological, geochemical, and mineralogical settings (Afzal et al., 2016; Carranza, 2009; Daneshvar Saein et al., 2012; Goncalves et al., 2001; Gumiel et al., 2010; Soltani et al., 2014). Famous fractal models include number–size (N-S: Mandelbrot, 1983; Sadeghi et al., 2012), concentration-area (C-A: Cheng et al., 1994), spectrum-area (S-A: Cheng et al., 1999), concentration- distance (C-D: Li et al., 2003), concentration–volume (C-V: Afzal et al., 2011), concentration-number (C-N: Hassanpour and Afzal, 2013), and simulated size–number (SS–N: Sadeghi et al., 2015).

Concentration-volume fractal models has been widely used in porphyry deposit (e.g. Afzal et al., 2011; Yasrebi et al., 2013; Soltani et al., 2014; Sun and Liu, 2014) and lesser another type of deposit such as gold deposit (Afzal et al., 2013; Lin et al., 2014), Zn-Pb MVT deposit (Delavar et al., 2012), iron deposit (Sadeghi et al., 2012; Afzal et al., 2015; Rahmati et al., 2015). Grade distribution of block

Citation info: Hajsadeghi, S., Asghari, O., Mirmohammadi, M., Afzal, P., Meshkani, A. A. 2020. Uncertainty-volume fractal model for delineating copper mineralization controllers using geostatistical simulation in Nohkouhi volcanogenic massive sulfide deposit, Central Iran. . Bulletin of the Mineral Research and Exploration, 161, 1-11. https://doi.org/10.19111/bulletinofmre.495753

* *Corresponding author: Omid ASGHARİ, o.asghari@ut.ac.ir*

models can be generated by geostatistical methods such as the Ordinary Kriging, Multi-Gaussian Kriging and Sequential Gaussian simulation. Geostatistical simulations are designed to overcome the smoothing effect of estimation methods (such as ordinary kriging and simple kriging) (e.g., Chiles and Delfiner, 2009). These methods are applied to continuous and indicator variables of respectively sequential Gaussian simulation (SGS e.g., Deutsch and Journel, 1998) and sequential indicator simulation (SIS e.g., Journel, 1983). Recently, geological phenomena e.g., mineralization, and alteration are separated effectively by combining simulation methods with fractal modeling (Afzal et al., 2014; Soltani et al., 2014; Sadeghi et al,. 2015).

The main aim of this paper was to indicate the relationship between copper grade, the probability of occurrence of copper ore minerals and host rocks in a VMS deposit. For this purpose, C-V fractal model was applied to Cu realizations produced from sequential Gaussian simulation. Also, U-V fractal model was used to distinguish different probability zones in two copper minerals of Nohkouhi deposit (i.e. chalcopyrite and malachite) using sequential indicator simulation.

2. Regional Geology of Mineral Deposit

The Nohkouhi copper deposit is located in Posht- e-Badam block as a part of Central Iran microcontinent (Figure 1a). This deposit contains 1.5 Mt measured of ore at average grades of 1% Cu (Karmania, 2013). Black shale and rhyodacite are main host of copper mineralization (Figure 1b). Based on Hajsadeghi et al (2017) studies copper mineralization occurred during three stages. Firstly, pyrite and minor chalcopyrite are deposited in the black shale, synchronously (Figure 2a, b, c). Second stage occurred during intrusion of rhyodacite in black shale. Copper enriched in black shale as a result of circulation of hydrothermal fluid (Figure 2d). Chalcopyrite formed as semi massive and veinlet with euhedral pyrite, lesser sphalerite and galena. During third stage, sulfide minerals oxidized and produced malachite, limonite, goethite, hematite ± azurite ± gypsum.

3. Applied Methods

3.1. Concentration-Number Fractal Model

Concentration- number (C-N) fractal model is one of the fractal models (Mandelbort, 1983) which it is used to separate geochemical background and anomaly in a geochemical dataset. The model is defined as (1):

$$N(\geq\rho) \infty \rho^{-\beta} \quad (1)$$

where N (≥ρ) denotes the sample number with concentration values greater than ρ value. ρ is

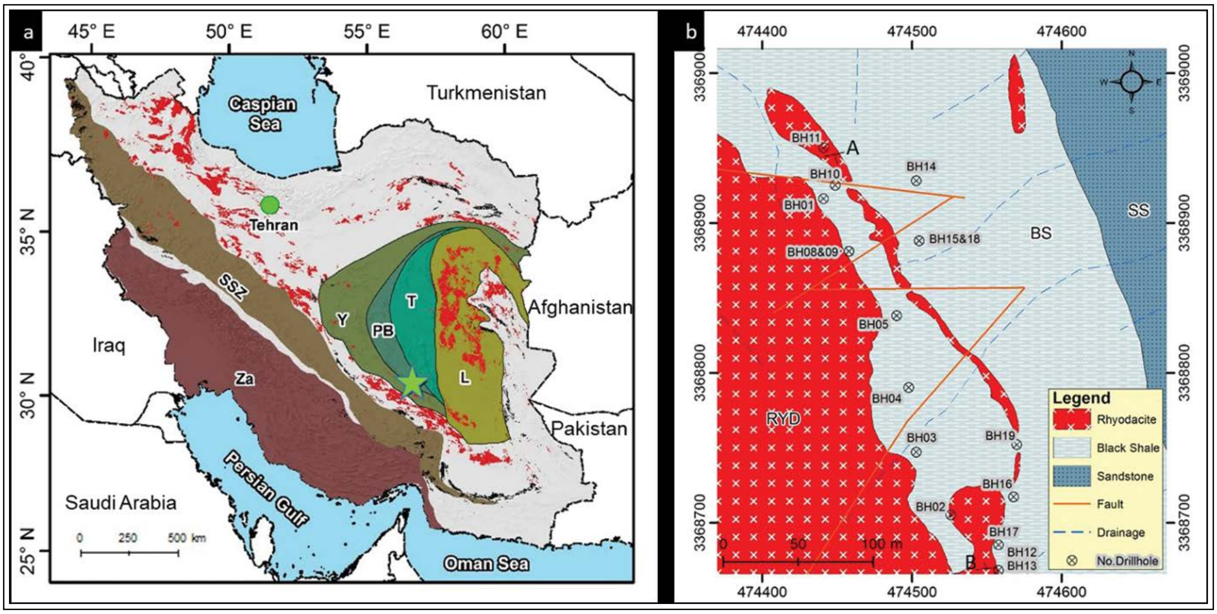

Figure 1- a) The location of Nohkouhi deposit in the regional geology map of Iran (Green stars; Simplified from Sahandi et al., 2002), b) Geology of the Nohkouhi deposit. Abbreviations: SSZ = Sanandaj-Sirjan zone, Za = Zagros, Y = Yazd block, PB = Posht-e-Badam block, T = Tabas block, L = Lut block.

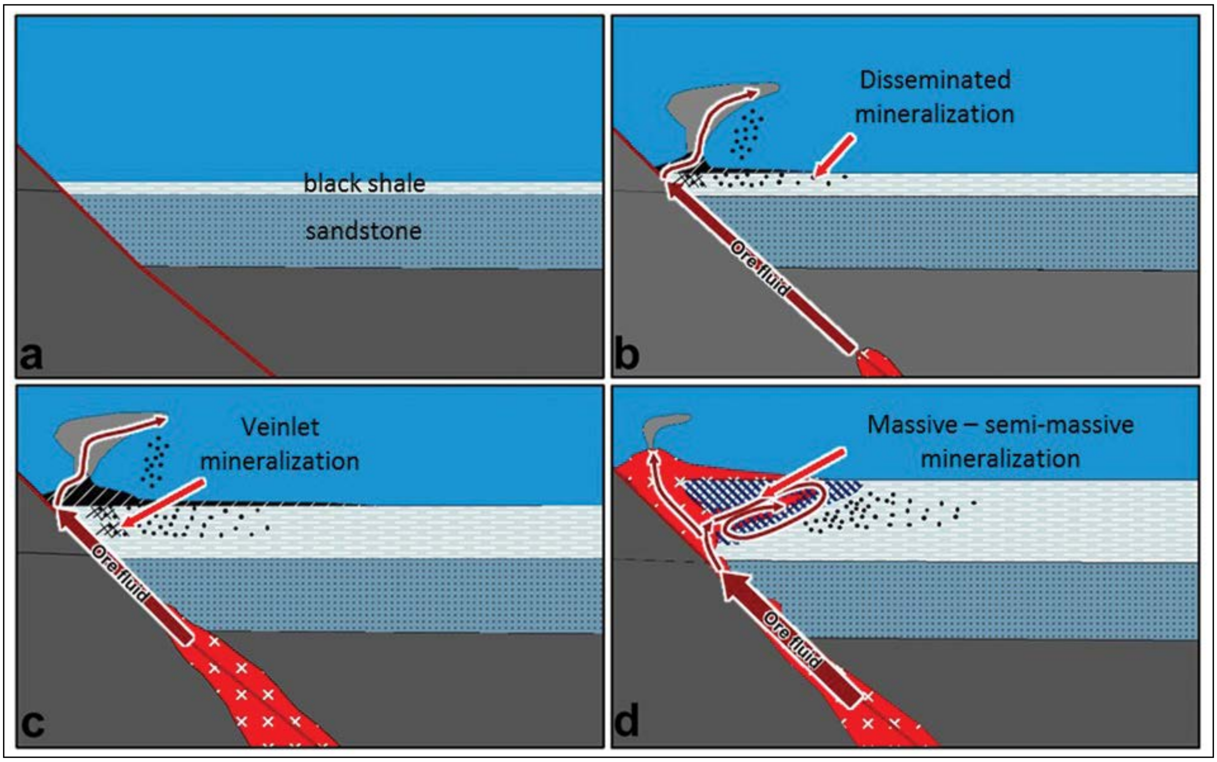

Figure 2- Schematic block diagram illustrating the most probable geodynamic scenario of the formation of Nohkouhi deposit (Hajsadeghi et al., 2017), a) sandstone and barren black shale are deposited, b-c) black shale and pyrite rich ± chalcopyrite had been deposited synchronously during first stage of mineralization while felsic magma ascended to the ground, d) copper mineralization is enriched as a result of circulation of magmatic fluid (second stage).

concentration of element, and β is the fractal dimension. The main advantage of this method is classification of geochemical populations before their estimation (Sadeghi et al., 2012; Rezaei et al., 2015).

3.2. Concentration-Volume (C-V) Fractal Model

The C-V fractal model was first introduced by Afzal et al. (2011) for separation of mineralization host rocks in different types of ore deposits. It has to be added here that in the C- V model, “C” can be replaced by either “concentration” (e.g. grade, or tonnage), or “probability” (e.g. uncertainty). In this paper, the researchers used “C” to refer to concentration. C- V fractal model can be expressed as:

$$V(c \leq \nu) \propto c^{-a1};\ V(c > \nu) \propto c^{-a2} \quad (2)$$

where $V(c \leq \nu)$ and $V(c > \nu)$ indicate volumes (V) with concentration values (c) smaller and greater than contour values (ν), respectively; a1 and a2 are characteristic exponents.

3.3. Sequential Gaussian Simulation

Sequential Gaussian simulation (SGS) is a conditional simulation of continuous variable (Goovaerts, 1996; Chiles and Delfiner, 1999). In this algorithm, data are transformed to a Gaussian distribution with a zero mean and a unit variance. In this method, hard data are obtained by moving conditioning data to the nearest grid nodes. The other nodes are simulated and considered as soft data. The procedure of sequential Gaussian simulation is as follows:

- Simulated node is randomly selected in the grid (1st randomness);
- Simulated value is selected from interval calculated from zero-realization (2nd randomness);
- Final histogram and distribution in each realization can be calculated from both hard and soft data:

$$Z^*_{SGS}=Z^*_{SK} +/- s_K(U) \quad (3)$$

where Z^*_{SK} calculate from simple kriging estimate; $s_K(U)$ signifies standard deviation of kriging estimate; and (U) is a random value from normal function and Z^*_{SGS} is simulated value (Rossi and Deutsch, 2013).

3.4. Sequential Indicator Simulation

Sequential indicator simulation (SIS) is deployed for categorical variables (e.g., Journel and Isaaks 1984). The realization is achieved through the following procedure:

- A random path is defined through the grid nodes to be simulated (target nodes). This part also includes data points (data nodes);
- Conditional cumulative distribution function is determined (ccdf) by the Indicator Kriging;
- Order relations is corrected to build a complete ccdf model;
- A simulation value draw from the corrected ccdf;
- Add the simulated value to the conditioning dataset;
- Proceed to the next node on the random path and repeat the above steps.

4. Experimental Dataset

The dataset consists of 559 rock samples with intervals of 2m gathered from 17 drill holes. The drill holes locations are provided on the geological map (Figure 1b). Drill hole samples were analyzed for 26 elements (Table 1) using inductively coupled plasma optical emission spectrometry (ICP-OES).

The copper grade histogram and C-N log-log plots for Cu were generated as depicted in figure 3a and 3b. Based on C-N fractal model, there are six populations for Cu. The first population for Cu appeared at grades below 160 ppm. The second population occurred between grades 160 ppm and 900 ppm. These populations are related to black shale and rhyodacite with very weak mineralization (Figure 3c).

The third and fourth populations are related to low grade mineralization in rhyodacite and black shale (Figure 3d), ranging between 900 to 3100 ppm and 3100 to 6300 ppm, respectively. The fifth population included major Cu mineralization which occurred in Cu grades between 6300 and 17800 ppm (Figure 3e). Eventually, the sixth population for the C-N log-log plot of Cu illustrates both extreme mineralization (Figure 3f) and enrichment in samples with Cu values higher than 17800 ppm.

5. C-V Fractal Modeling of Copper Grade Based on SGS

Sequential Gaussian simulation was used for generating 10 realizations of the copper grade. Nohkouhi deposit is simulated using 600.000 cells, which have a cell dimension of 2 m×2 m×2 m in the X, Y, and Z directions, respectively.

The grade data are transformed into Gaussian distribution, on which the semi-variogram analysis is performed. Due to the lack of boreholes in azimuth 70^o, no experimental variogram has been obtained. Hence, based on geological knowledge (e.g. ratio between structural axis), the range of the second direction (Az 70^o) was considered equal to 75% of the range of the major axis.

Consequently, the following semi-variogram model, consisting of a nugget effect and a nested spherical model, was obtained (Figure 4):

Table 1- Detection limits for analyzed elements.

Element	Ag	Al	As	Ca	Cd	Ce	Co	Cr	Cu	Fe	La	Li	Mg
Unit	ppm	ppm	ppm	ppm	ppm	ppm	ppm	ppm	ppm	ppm	ppm	ppm	ppm
Detection limit	0,1	100	0,5	100	0,1	1	1	1	1	100	1	1	100
Element	Mn	Mo	Ni	P	Pb	S	Sb	Sc	Th	V	Y	Yb	Zn
Unit	ppm	ppm	ppm	ppm	ppm	ppm	ppm	ppm	ppm	ppm	ppm	ppm	ppm
Detection limit	5	0,5	1	5	1	50	0,5	0,5	0,5	1	0,5	0,2	1

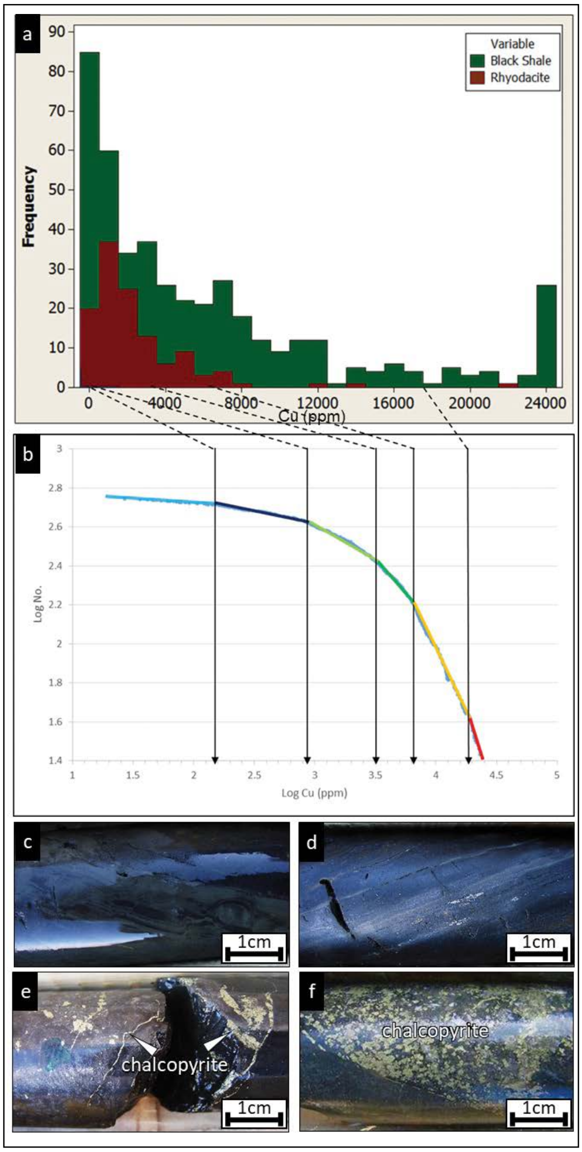

Figure 3- a) Histogram of Cu, b) C-N log-log plot for Cu concentrations in Nohkouhi deposit, c) barren black shale, d) disseminated chalcopyrite, e) veinlet of chalcopyrite, f) Massive-semi-massive chalcopyrite hosted by black shale.

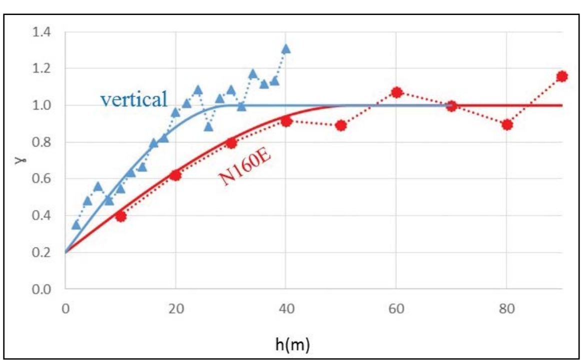

Figure 4- Experimental (dashed lines) and theoretical (solid lines) semi variograms along major (N160E) and minor (vertical) anisotropy axis (Gaussian transformed grade data).

$$\gamma_{N160E} = 0.2 \text{ nugget} + 0.8 \text{ Sph } (52) \qquad 4$$

$$\gamma_{N070E} = 0.2 \text{ nugget} + 0.8 \text{ Sph } (40) \qquad 5$$

$$\gamma_{horizental} = 0.2 \text{ nugget} + 0.8 \text{ Sph } (32) \qquad 6$$

where the distances into brackets denote the ranges along each directions.

Thresholds values of simulated Cu grades were identified using C-V log-log plots of the simulations (Figure 5). The simulations indicate four or five populations with different thresholds, as depicted in figure 5 and table 2. The enriched zones in the different simulated data are higher than 2,23%. Moreover, the main mineralization of Cu commences from 0,5% for sim 1, 3, 6, 7, 8, 9, and 10. In addition, the major Cu mineralized zones occurred in Cu values greater than 0,3% in sim 2, 4 and 5. One can see that, there is similar threshold with minor difference between them. So just two realization will be investigated.

6. U-V Fractal Modeling Of Copper Mineralization Based On SIS

In this study, SIS is used to simulate two copper ore minerals of chalcopyrite and malachite, separately. Indicator variables for copper minerals are defined as:

$$I_{malachite} = \begin{cases} \textit{if malachite present} \\ \textit{0 other} \end{cases} \qquad 7$$

$$I_{chalcopyrite} = \begin{cases} \textit{1 if chalcopyrite present} \\ \textit{0 other} \end{cases} \qquad 8$$

The experimental variogram are fitted by nugget effect and spherical model (Figure 6). However, as in the previous section, due to the lack of boreholes in azimuth 70°, no experimental variogram has been obtained. So, the range of the second direction (Az 70°) was considered equal to 75% of the range of the major axis.

$$\text{chalcopyrite} = \begin{cases} \gamma_{K160E} = 0.02 \text{ nugget} + 0.18 \text{ Sph } (144) \\ \gamma_{K070E} = 0.02 \text{ nugget} + 0.18 \text{ Sph } (108) \\ \gamma_{vertical} = 0.02 \text{ nugget} + 0.18 \text{ Sph } (40) \end{cases} \qquad 9$$

$$\text{malachite} = \begin{cases} \gamma_{K160E} = 0.02 \text{ nugget} + 0.16 \text{ Sf } (200) \\ \gamma_{K070E} = 0.02 \text{ nugget} + 0.16 \text{ Sf } (150) \\ \gamma_{vertical} = 0.02 \text{ nugget} + 0.16 \text{ Sf } (21) \end{cases} \qquad 10$$

where the distances into brackets represent the ranges along the directions.

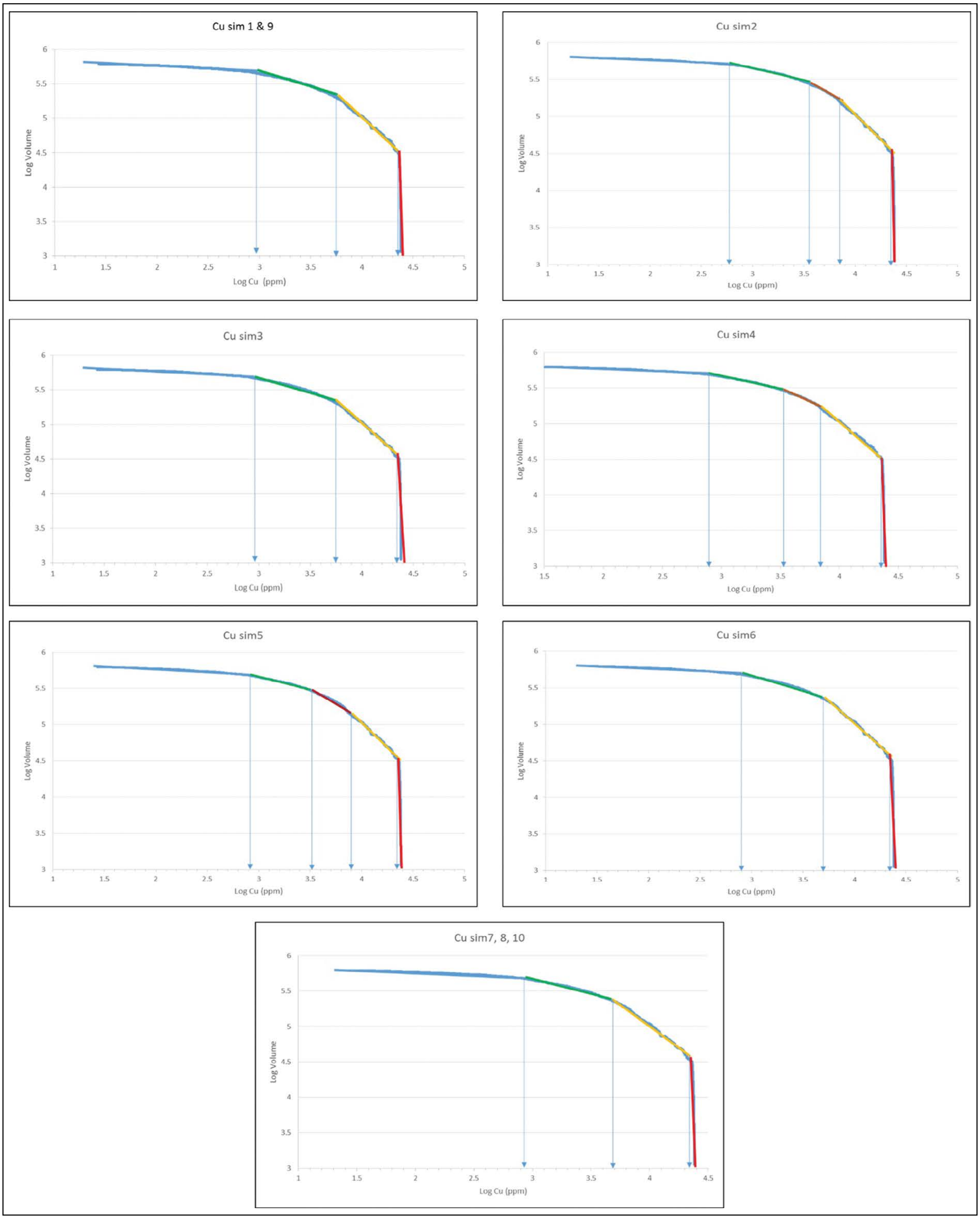

Figure 5- C-V log–log plots of different realizations of SGS and E-type.

Table 2- Cu threshold values (ppm) were recognized using C–V fractal model for different realizations.

Realization no.	First	Second	Third	Forth
Sim 1	1000	5623	22387	-
Sim 2	630	3548	7079	22387
Sim 3	891	5623	22387	-
Sim 4	794	3162	7079	22387
Sim 5	794	3162	7943	22387
Sim 6	794	5011	22387	-
Sim 7	891	5011	22387	-
Sim 8	891	5011	22387	-
Sim 9	1000	5623	22387	-
Sim 10	891	5011	22387	-

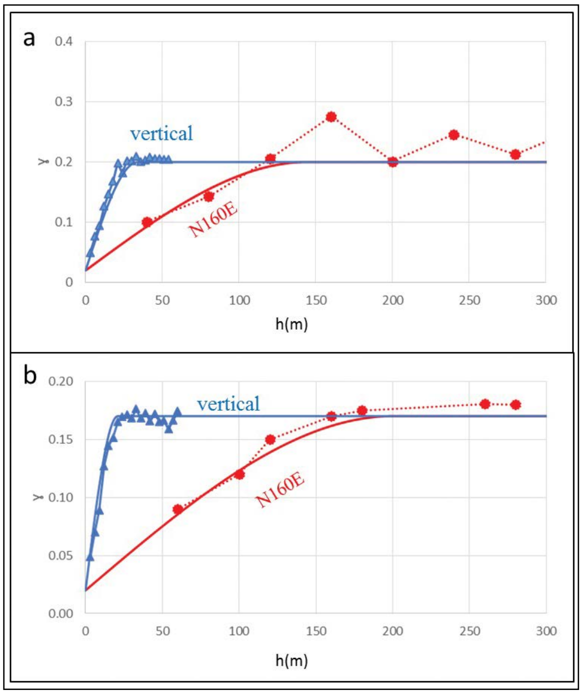

Figure 6- Sample (dashed lines) and modeled (solid lines) semi variograms along main anisotropy directions, a) chalcopyrite, b) malachite.

The probability maps of chalcopyrite and malachite were calculated and U-V fractal modeling was obtained for these ores. Threshold values were determined in the U-V log-log plot as breakpoints which reveal a power-law relationship between probability of minerals and the volumes occupied (Figure 7). Three breakpoints (0,13, 0,6, 0,83 and 0,13, 0,52, 0,83 for chalcopyrite and malachite respectively) appeared in the U-V log-log plots which represent four populations for chalcopyrite and malachite (Figure 7). As a result, the plots revealed four zones with variable probabilities, ranging from low to highly probable zones (Figure 8).

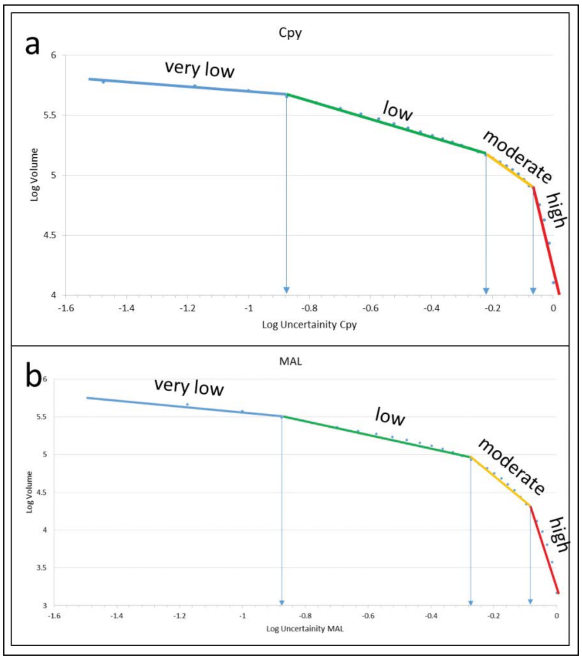

Figure 7- U–V log–log plots of copper ore minerals in the Nohkouhi deposit (Cpy: Chalcopyrite; Mal: Malachite).

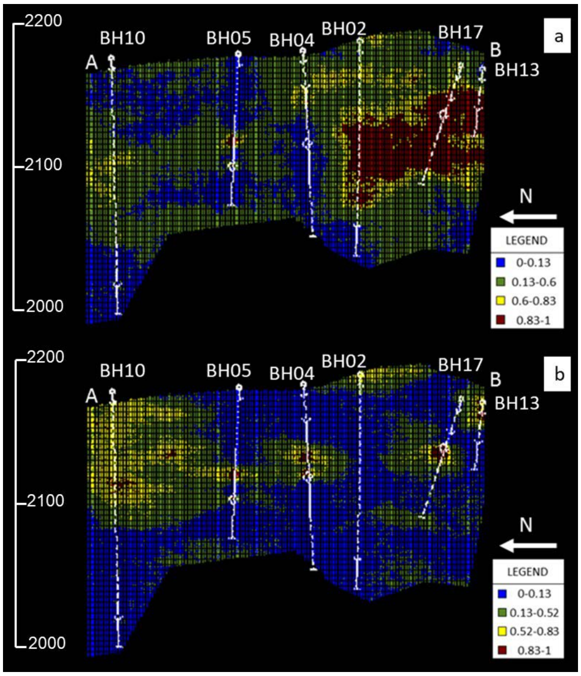

Figure 8- Different probability mineralization zones for a) chalcopyrite b) malachite based on the U–V fractal modeling and probability map of 30 realizations of copper ores. Section A-B is provided on figure 1.

7. Comparison of Fractal and Host Rock Models of the Deposit

The results derived from C-V fractal modeling of the deposit are correlated with U-V fractal model of copper minerals. Confusion matrix is utilized to calculate spatial correlations between the results provided by U-V and C-V fractal models (Table 3; Carranza, 2011). Due to similar results, only two realizations were reviewed (realization 1 and 10). Based on confusion matrix (Tables 4-5), generally, the realizations represent the proper results of a highly probable delineation (CPY≥0,83 and Mal

Table 3- Matrix for comparing performance of fractal modeling results with geological model. A, B, C, and D represent numbers of voxels in overlaps between classes in the binary geological model and the binary results of fractal models (Carranza, 2011).

		Geological model	
		Inside zone	Outside zone
Fractal model	Inside zone	True positive (A)	False positive (B)
	Outside zone	False negative (C)	True negative (D)
		Type I error = C/(A +C)	Type II error = B / (B + D)
		Overall accuracy =(A+D)/(A+B+C+D)	

Table 4- Overall accuracy (OA), Type I and Type II errors (T1E and T2E, respectively), resulted from U-V fractal models of copper minerals and C–V fractal modeling of realizations 1.

	CPY ≥ 0,83			0,6 ≤ CPY < 0,83			0,13 ≤ CPY < 0,6			CPY < 0,13	
Cu ≥ 22387	A	B	5623≤ Cu<22387	A	B	1000 ≤ Cu<5623	A	B	Cu < 1000	A	B
	5484	76172		18807	47278		122502	183239		49481	120350
	C	D		C	D		C	D		C	D
	28372	513285		153233	403995		120559	187688		121067	332414
	OA	0,83		OA	0,67		OA	0,50		OA	0,61
	ETI	0,83		ETI	0,89		ETI	0,49		ETI	0,70
	ETII	0,13		ETII	0,11		ETII	0,49		ETII	0,26
	Mal ≥ 0,83			0,52 ≤ Mal < 0,83			0,13 ≤ Mal < 0,52			Mal < 0,13	
Cu ≥ 22387	A	B	5623≤ Cu<22387	A	B	1000≤ Cu<5623	A	B	Cu < 1000	A	B
	2772	14651		27082	41265		87388	137662		111560	200933
	C	D		C	D		C	D		C	D
	31084	574806		144958	410008		159481	238782		58988	251831
	OA	0,92		OA	0,70		OA	0,52		OA	0,58
	ETI	0,91		ETI	0,84		ETI	0,64		ETI	0,34
	ETII	0,02		ETII	0,09		ETII	0,36		ETII	0,44

Table 5- Overall accuracy (OA), Type I and Type II errors (T1E and T2E, respectively), resulted from U-V fractal models of copper minerals and C–V fractal modeling of realizations 10.

	CPY ≥ 0,83			0,6 ≤ CPY < 0,83			0,13 ≤ CPY < 0,6			CPY < 0,13	
Cu ≥ 22387	A	B	5011 ≤ Cu < 22387	A	B	891 ≤ Cu < 5011	A	B	Cu < 891	A	B
	1820	79836		21417	44668		119453	186288		33030	136801
	C	D		C	D		C	D		C	D
	32036	509621		170285	386943		118973	189274		122538	330944
	OA	0,82		OA	0,66		OA	0,50		OA	0,58
	ETI	0,95		ETI	0,89		ETI	0,50		ETI	0,79
	ETII	0,14		ETII	0,10		ETII	0,50		ETII	0,29
	Mal ≥ 0,83			0,52 ≤ Mal < 0,83			0,13 ≤ Mal < 0,52			Mal < 0,13	
Cu ≥ 22387	A	B	5011≤ Cu < 22387	A	B	891≤ Cu < 5011	A	B	Cu < 891	A	B
	1847	15576		28187	40160		82580	142470		90390	222103
	C	D		C	D		C	D		C	D
	32009	573881		163515	391451		159607	238656		65178	245642
	OA	0,92		OA	0,67		OA	0,52		OA	0,54
	ETI	0,95		ETI	0,85		ETI	0,66		ETI	0,42
	ETII	0,03		ETII	0,09		ETII	0,37		ETII	0,47

≥0,83). Moreover, C–V modeling of realizations is appropriate for moderate probability (0.6≤CPY<0.83 and 0,52≤Mal<0,83). On the other hand, C–V fractal modeling provides relatively poor results for low and very low probabilities (0,13≤CPY<0,6, CPY<0,13, 0,13≤Mal<0,52, Mal<0,13) of copper minerals. Hence, this finding can be used to show the relationship between two probability zones (i.e. high and moderate) and copper grades. 3D models of the rock types (black shale, rhyodacite, and sandstone) were generated by employing SIS and geological drill core data (Hajsadeghi et al., 2016). Figure 9a displays the most frequently occurring model of rock types.

Merging C-V and U-V fractal models with the most frequent model of rock types helps delineate different copper populations in this deposit (Figure 9). Based on the log–log plots, Cu concentrations in massive, semi-massive, and oxide zones, hosted by black shale and partly by rhyodacite, are shown to be greater than 22387 ppm. The disseminated and veinlet zones have a concentration range varying between 5011 and 7943 ppm. This zone is hosted by black shale and rhyodacite. Besides, it was observed that low-grade host rocks had a Cu concentration between 1000 and 5011 ppm which is hosted by both of the host rocks. Finally, the barren part of all three host rocks (black shale, rhyodacite, and sandstone) is characterized by a Cu concentration lower than 1000 ppm. Geostatistical-fractal simulations conform to the hydrothermal and mineralization process of Nohkouhi copper deposit.

8. Conclusion

C-V fractal model revealed different copper grade mineralization's which are related to various copper ores and accumulations in Nohkouhi VMS deposit. U-V fractal model was used to obtain different probability zones for occurrence of copper minerals. C-V fractal modeling provided four or five populations. Several copper populations were delineated based on the results of U-V and C–V fractal modeling and the most frequently occurring model of rock types. Massive, semi-massive, and oxide zones - hosted by black shale

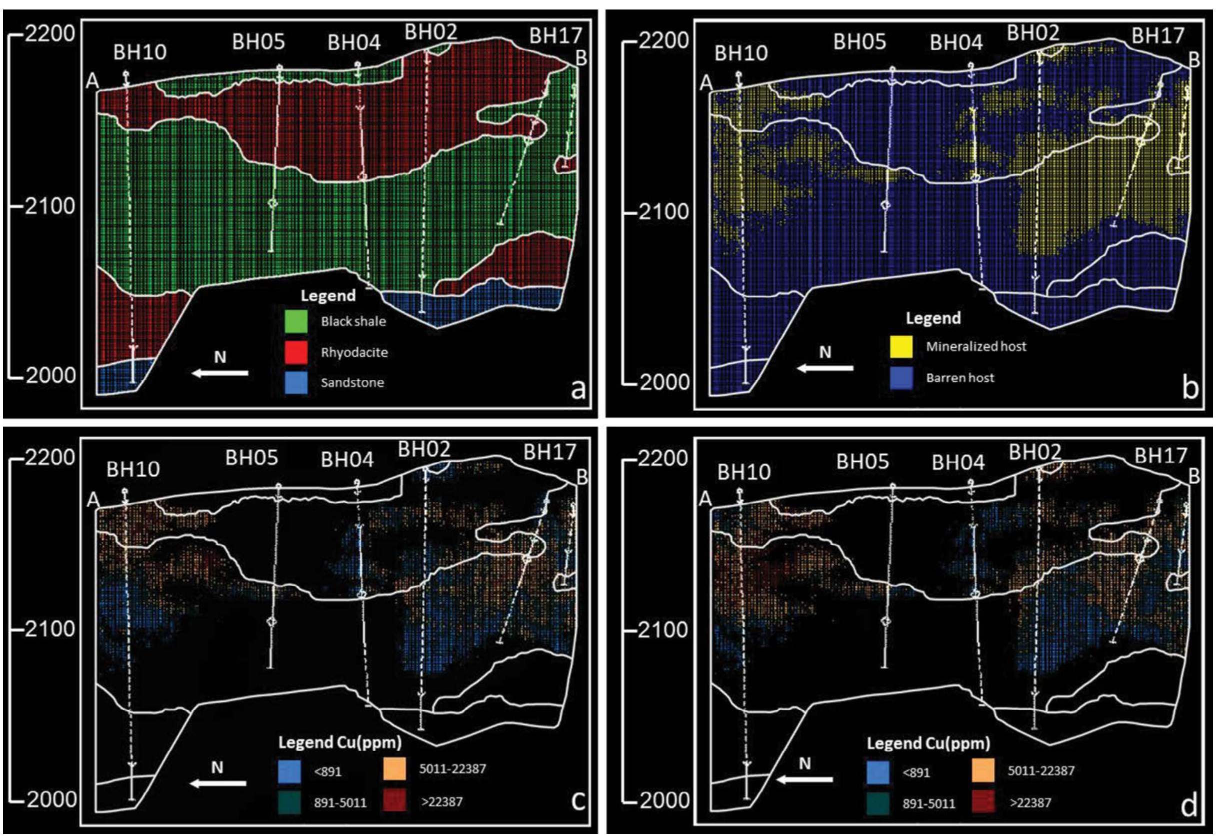

Figure 9- a) Most frequent occurrence model of rock types obtained by SIS (Hajsadeghi et al., 2016), b) Mineralized host rock characterized by MAL> 0.52 or CPY> 0.6, c) different Cu populations based on C–V fractal modeling in a simulation in realization 1, d) different Cu populations based on C–V fractal modeling in a simulation in realization 10. Section A-B is provided on figure 1.

were found to be higher than 2,24%. The disseminated and veinlet zones, hosted by black shale and rhyodacite, each showed a concentration range of 1,99-2,24% and 0,31-0,56%, respectively. Additionally, low-grade host rocks, occurring in black shale and rhyodacite, exhibited a Cu concentration ranging between 0.1-0,31 %. Eventually, the barren part of all host rocks, consisting of black shale, rhyodacite, and sandstone, were featured by a Cu concentration lower than 0.1%. These are related to characterize of Nohkouhi VMS deposit which suggested in pervious study (Hajsadeghi et al., 2017). However a 3D model can be more useful in exploration than a simple schematic model.

Acknowledgments

The authors are grateful to Zarmesh Group for providing the dataset used in this study.

References

Afzal, P., Alghalandis, Y.F., Khakzad, A., Moarefvand, P., Omran, N.R. 2011. Delineation of mineralization zones in porphyry Cu deposits by fractal concentration–volume modeling. Journal of Geochemical Exploration 108(3), pp.220-232.

Afzal, P., Ahari, H.D., Omran, N.R., Aliyari, F. 2013. Delineation of gold mineralized zones using concentration–volume fractal model in Qolqoleh gold deposit, NW Iran. Ore Geology Reviews 55, pp.125-133.

Afzal, P., Alhoseini, S.H., Tokhmechi, B., Ahangaran, D.K., Yasrebi, A.B., Madani, N., Wetherelt, A. 2014. Outlining of high quality coking coal by concentration–volume fractal model and turning bands simulation in East-Parvadeh coal deposit, Central Iran. International Journal of Coal Geology 127, pp.88-99.

Afzal, P., Madani, N., Shahbeik, S., Yasrebi, A.B. 2015. Multi-Gaussian kriging: a practice to enhance delineation of mineralized zones by Concentration–Volume fractal model in Dardevey iron ore deposit, SE Iran. Journal of Geochemical Exploration 158, pp.10-21.

Afzal, P., Tehrani, M.E., Ghaderi, M., Hosseini, M.R. 2016. Delineation of supergene enrichment, hypogene and oxidation zones utilizing staged factor analysis and fractal modeling in Takht-e-Gonbad porphyry deposit, SE Iran. Journal of Geochemical Exploration, 161, pp.119-127.

Carranza, E.J.M. 2009. Controls on mineral deposit occurrence inferred from analysis of their spatial pattern and spatial association with geological features. Ore Geology Reviews 35(3), pp.383-400.

Carranza, E.J.M. 2011. Analysis and mapping of geochemical anomalies using logratio-transformed stream sediment data with censored values. Journal of Geochemical Exploration 110(2), pp.167-185.

Cheng, Q. 1999. Spatial and scaling modelling for geochemical anomaly separation. Journal of Geochemical Exploration 65(3), pp.175-194.

Cheng, Q., Agterberg, F.P., Ballantyne, S.B. 1994. The separation of geochemical anomalies from background by fractal methods. Journal of Geochemical Exploration 51(2), pp.109-130.

Chilés, J.P., Delfiner, P. 2012. Geostatistics: modeling spatial uncertainty (Vol. 497). John Wiley & Sons.

Daneshvar Saein, L., Rasa, I., Rashidnejad Omran, N., Moarefvand, P., Afzal, P. 2012. Application of concentration-volume fractal method in induced polarization and resistivity data interpretation for Cu-Mo porphyry deposits exploration, case study: Nowchun Cu-Mo deposit, SE Iran. Nonlinear Processes in Geophysics 19(4), pp.431-438.

Delavar, S.T., Afzal, P., Borg, G., Rasa, I., Lotfi, M., Omran, N.R. 2012. Delineation of mineralization zones using concentration–volume fractal method in Pb–Zn carbonate hosted deposits. Journal of Geochemical Exploration 118, pp.98-110.

Deutsch, C.V., Journel, A.G. 1998. Geostatistical software library and user's guide. Oxford University Press, New York.

Goncalves, M.A., Mateus, A., Oliveira, V. 2001. Geochemical anomaly separation by multifractal modelling. Journal of Geochemical Exploration 72(2), pp.91-114.

Goovaerts, P. 1996. Geostatistics for natural resources evaluation. Oxford University Press on Demand.

Gumiel, P., Sanderson, D.J., Arias, M., Roberts, S. Martín-Izard, A. 2010. Analysis of the fractal clustering of ore deposits in the Spanish Iberian Pyrite Belt. Ore Geology Reviews 38(4), pp.307-318.

Hajsadeghi, S., Asghari, O., Mirmohammadi, M., Meshkani, S.A. 2016. Indirect rock type modeling using geostatistical simulation of independent components in Nohkouhi volcanogenic massive sulfide deposit, Iran. Journal of Geochemical Exploration 168, pp.137-149.

Hajsadeghi, S., Mirmohammadi, M., Asghari, O., Meshkani, S.A. 2017. Geology and mineralization at the copper-rich volcanogenic massive sulfide deposit in Nohkouhi, Posht-e-Badam block, Central Iran. Ore Geology Review doi:https://doi.org/10.1016/j.oregeorev.2017.11.030.

Hassanpour, S., Afzal, P. 2013. Application of concentration–number (C–N) multifractal modeling for geochemical anomaly separation in Haftcheshmeh porphyry system, NW Iran. Arabian Journal of Geosciences 6(3), pp.957-970.

Journel, A.G. 1983. Nonparametric estimation of spatial distributions. Journal of the International Association for Mathematical Geology 15(3), pp.445-468.

Journel, A.G., Isaaks, E.H. 1984. Conditional indicator simulation: Application to a Sachatchewan uranium deposits. Marhematical Geology 16 (7):685-718.

Karmania, A. 2013.Company, Preliminary Exploration Report in Nohkouhi Area, Tehran (73 pp., (In Persian)).

Li, C., Ma, T., Shi, J. 2003. Application of a fractal method relating concentrations and distances for separation of geochemical anomalies from background. Journal of Geochemical Exploration 77(2), pp.167-175.

Lin, X., Zhang, B., Wang, X. 2014. Application of factor analysis and concentration-volume fractal modeling to delineation of 3D geochemical patterns: a case study of the Jinwozi gold field, NW China. Geochemistry: Exploration, Environment, Analysis 14(4), pp.359-367.

Mandelbrot, B.B. 1983. The fractal geometry of nature (Vol. 173). Macmillan.

Rahmati, A., Afzal, P., Abrishamifar, S.A., Sadeghi, B. 2015. Application of concentration–number and concentration–volume fractal models to delineate mineralized zones in the Sheytoor iron deposit, Central Iran. Arabian Journal of Geosciences 8(5), pp.2953-2965.

Rezaei, S., Lotfi, M., Afzal, P., Jafari, M.R., Meigoony, M.S. 2015. Delineation of Cu prospects utilizing multifractal modeling and stepwise factor analysis in Noubaran 1: 100,000 sheet, Center of Iran. Arabian Journal of Geosciences 8(9), pp.7343-7357.

Rossi, M.E., Deutsch, C.V. 2013. Mineral resource estimation. Springer Science & Business Media.

Sadeghi, B., Moarefvand, P., Afzal, P., Yasrebi, A.B., Saein, L.D. 2012. Application of fractal models to outline mineralized zones in the Zaghia iron ore deposit, Central Iran. Journal of Geochemical Exploration 122, pp.9-19.

Sadeghi, B., Madani, N., Carranza, E.J.M. 2015. Combination of geostatistical simulation and fractal modeling for mineral resource classification. Journal of Geochemical Exploration 149, pp.59-73.

Sahandi, M. R., Soheily, M., Sadeghi, M., Delavar, S.T., Jafari Rad, A. 2002. Geological Map of Iran, 1:1,000,000. Geological Survey of Iran, Tehran, Unpublished

Soltani, F., Afzal, P., Asghari, O. 2014. Delineation of alteration zones based on Sequential Gaussian Simulation and concentration–volume fractal modeling in the hypogene zone of Sungun copper deposit, NW Iran. Journal of Geochemical Exploration 140, pp.64-76.

Sun, T., Liu, L. 2014. Delineating the complexity of Cu–Mo mineralization in a porphyry intrusion by computational and fractal modeling: A case study of the Chehugou deposit in the Chifeng district, Inner Mongolia, China. Journal of Geochemical Exploration 144, pp.128-143.

Yasrebi, A.B., Afzal, P., Wetherelt, A., Foster, P., Esfahanipour, R. 2013. Correlation between geology and concentration-volume fractal models: significance for Cu and Mo mineralized zones separation in the Kahang porphyry deposit (Central Iran). Geologica Carpathica 64(2), pp.153-163.